Available online at www.sciencedirect.com
ScienceDirect
Composites Science and Technology 68 (2008) 658–665
COMPOSITES SCIENCE AND TECHNOLOGY
www.elsevier.com/locate/compscitech

Enhancement of through-thickness thermal conductivity in adhesively bonded joints using aligned carbon nanotubes

Sangwook Sihn [a,*], Sabyasachi Ganguli [b], Ajit K. Roy [c], Liangti Qu [d], Liming Dai [d]

[a] University of Dayton Research Institute, 300 College Park, Dayton, OH 45469-0060, USA
[b] Research Associate, National Research Council, Washington, DC, USA
[c] Air Force Research Laboratory, Wright-Patterson AFB, OH 45433-7750, USA
[d] University of Dayton, 300 College Park, Dayton, OH 45469, USA

Received 20 March 2007; received in revised form 21 August 2007; accepted 20 September 2007
Available online 29 September 2007

Abstract

A concept of incorporating aligned multi-walled carbon nanotubes (MWCNTs) in the adhesive layer has been demonstrated to enhance the through-thickness thermal conductivity in the adhesively bonded joints. Both numerical and experimental studies were performed to determine key components in improving the through-thickness thermal conductivity and to realize the improvement in an adhesively-jointed system. The numerical analysis indicated that the key components to improve the through-thickness thermal conductivity in the adhesive joints are using highly conductive vertically aligned nanotubes as well as the thermal conductivity and the size of a transition zone between the nanotube ends and surrounding matrix materials in the form of either the adhesive or adherends. Therefore, the thermal contact of the conductive phase (the MWNT in this case) with the adherent surfaces is essential to achieve the desirable through-thickness thermal conductivity in joints. This theoretical observation was demonstrated experimentally by using conductive graphite facesheets as adherends and the polymer adhesive layer with the aligned MWCNTs. To ensure the ends of the MWCNTs make thermal contact with the adherent surfaces, the surface of the adhesive with the MWCNTs were plasma-etched and coated with thin Au layer, along with the surface of the graphite facesheet coated with thin Au–Pd layer. The measured value of the through-thickness thermal conductivity of the modified adhesive joint with the MWNCT was over 250 W/m K, which superseded the thermal conductivity of neat adhesive joint by several order of magnitudes. Thus the study demonstrates a new approach as well as opportunities of much needed thermal property tailoring in structural joints.

Keywords: A. Adhesive joints; A. Nanostructures; B. Thermal properties; C. Finite element analysis (FEA); E. Chemical vapour deposition (CVD)

1. Introduction

Based on a current requirement of space industries, a through-thickness thermal conductivity (k_z) of adhesive of about 7–10 W/m K is expected to enable efficient multi-functionality and lean manufacturing of systems to numerous applications, ranging from electronic cooling, efficient space structures, and to dramatically improving the energy conversion efficiency of the directed energy devices. The through-thickness thermal conductivity in adhesive joints currently in use severely lacks to meet the requirement mentioned above. One of the barriers in achieving adequate through-thickness thermal conductivity in composite materials and also in composite joints is due to the extremely low thermal conductivity of matrix resins or adhesives (typically $k_z \sim 0.3$ W/m K). The poor thermal conductivity of resin and/or adhesives fails to meet the needed k_z at the system level, as structural components are primarily assembled through bonded joints. A possible concept of enhancing through-thickness thermal conductivity in the adhesive joints is to incorporate carbon nanotubes (CNTs) in the adhesive layer.

* Corresponding author. Tel.: +1 937 255 9324; fax: +1 937 258 8075.
E-mail address: sangwook@stanfordalumni.org (S. Sihn).

0266-3538/$ - see front matter © 2007 Elsevier Ltd. All rights reserved.
doi:10.1016/j.compscitech.2007.09.016

Various unique properties of the CNTs have generated interest among many researchers over the last decade [1]. These researchers have reported remarkable electrical [2], mechanical [3], and thermal properties [4] related to their unique structure and high aspect ratio. These unique properties make CNTs the material of choice for numerous applications like sensors [5], actuators [6], energy storage devices [7], and nanoelectronics [8]. The CNTs also have extremely high thermal conductivity in the axial direction [9]. According to molecular dynamics simulations, the value can reach as high as 6500 W/m K at room temperature for single-walled CNTs (SWCNTs). Researchers have experimentally determined the thermal conductivity of multi-walled CNTs (MWCNTs) to be 2000–3000 W/m K at room temperature [10]. This outstanding thermal property of nanotubes has made them target materials for thermal management materials. Thermal conductivity enhancement has been observed in nanotube suspensions [11]. The results were theoretically intriguing as the measured thermal conductivities were abnormally greater than theoretical predictions with conventional heat conduction models [12]. Biercuk, et al. [13] measured thermal transport properties of industrial epoxy loaded with as-produced SWCNTs (>5 wt.%) from 20 to 300 K. It was observed that samples with 1% unpurified SWCNT material showed a 125% increase in thermal conductivity at room temperature. Unpurified CNTs were introduced to silicone elastomer to investigate their effect on the thermal conductivity [14]. The measured values of the thermal conductivity were found to increase with the carbon amount. There was a 65% enhancement in the thermal conductivity with 3.8 wt.% CNT loading. Thermal interface materials (TIM) used for dissipating heat efficiently from electronic components is gaining increased attention. Thermal conducting pads made with various conductive fillers are widely used commercially. The CNTs with their exceptional thermal properties are an ideal candidate for TIM applications. Huang et al. [15] developed TIM based on aligned CNT embedded in an elastomer. Though they achieved a 120% enhancement of thermal conductivity using the nanocomposite film, the achieved value of 1.21 W/m K was much less than the theoretical thermal conductivity of aligned CNTs.

As stated above, the thermal conductivity of MWCNT is on the order of 2000 W/m K, which is large in comparison to that of the adhesive (~0.3 W/m K). Hence, the acoustic impedance, which is proportionally related to the thermal conductivity, of MWCNT is much higher than that of the adhesive. It is known that the phonon transmission coefficient (hence, the thermal conductivity) at the interface of dissimilar materials (MWCNT and adhesive in this case) is critically affected by the acoustic impedance mismatch between the respective materials [16]. For this particular reason, the approach of mixing CNTs or nanofibers in adhesive, exhibiting large impedance mismatch between the CNT ends and adhesive, only marginally improved its thermal conductivity to approximately 0.7 W/mK [13–15], which fails to provide an adequate solution for this study. Furthermore, the interfacial imperfections between the adhesive material and adherends degrade the thermal transfer efficiency significantly. Thus to improve phonon transport through the adhesive joints, the mismatch of the acoustic impedance between the CNTs and the adhesive needs to be minimized.

In this study, an efficient adhesive joint system was developed to improve the through-thickness thermal conductivity. We used vertically aligned MWCNTs to improve the through-thickness thermal conductivity in adhesive joints. The thermal conductivity of the aligned MWCNTs is not known. However, it is expected that the thermal properties of the aligned MWCNTs are similar to those of the individual MWCNTs if the quality and chirality of the MWCNTs remain the same. Furthermore, we introduced a transition zone (TZ) at the interface between the MWCNTs and the surrounding material to minimize the impedance mismatch and thus to minimize the interfacial imperfections. Firstly, a numerical analysis based on a finite element (FE) analysis was conducted to study the effect of the nanotube and the TZ on the thermal transfer performance. Both geometric and thermal property variation were considered in parametric studies. Secondly, for validation of the FE simulation, the adhesive joint system was fabricated with the vertically aligned MWCNTs as well as the introduction of the TZ between the nanotube ends and the surrounding adhesive/adherend surfaces. The TZ was achieved experimentally between the nanotube ends and graphite adherend surfaces through a series of metallic coatings, after a suitable functionalization of nanotube ends and the adherend surfaces.

2. Numerical thermal analysis

2.1. Steady-state and transient thermal analysis

In order to understand the effect of the materials parameters on through-thickness thermal conductivity in the adhesive joint, as stated earlier, a continuum based FE thermal analysis of the adhesive joint was performed. Fig. 1 shows a schematic configuration of the present joint system. The vertically aligned MWCNTs (nanograss) are present in an adhesive layer that is placed between two adherent facesheets.

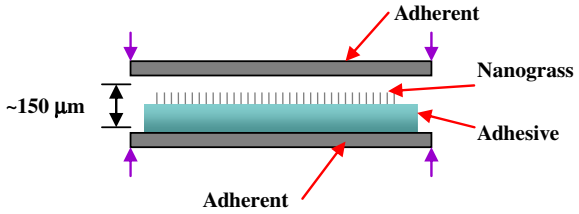

Fig. 1. Schematic configuration of the nanograss (MWCNTs) infiltrated with adhesive in adhesive joint.

A representative unit-cell model was developed in order to pinpoint critical parameters that significantly affect the through-thickness conductivity in the adhesive joint. The unit-cell model considers a single NT that is embedded in the adhesive matrix at the ends. The connection between the NT and the matrix was achieved with the TZ. The FE analysis discretely modeled the nanotube, matrix material surrounding the nanotubes and the TZ between the nanotube and matrix materials. Fig. 2 shows FE meshes for both straight and curved nanotubes embedded in matrix through the TZ. Typical diameter and length of the nanotube were selected to be 20 nm and 1 μm for the simulation, respectively. Steady-state and transient thermal analyses were conducted with the FE simulation by using a commercial FE software, ANSYS. Baseline properties of the thermal analysis were set as follows:

Nanotube :

$$k_{NT} = 500\ \mathrm{W/m\,K}, \quad \rho_{NT} = 1.5\ \mathrm{g/cm^3}, \quad C_{pNT} = 0.6\ \mathrm{J/g\,K},$$

Matrix :

$$k_{m} = 0.2\ \mathrm{W/m\,K}, \quad \rho_{m} = 1.6\ \mathrm{g/cm^3}, \quad C_{pm} = 1.3\ \mathrm{J/g\,K},$$

TZ :

$$k_{TZ} = 0.2\ \mathrm{W/m\,K}, \quad \rho_{TZ} = 1.6\ \mathrm{g/cm^3}, \quad C_{pTZ} = 1.3\ \mathrm{J/g\,K},$$

where k, ρ and C_p are thermal conductivity, density and heat capacity, respectively. The heat capacity of the nanotube was assumed to be similar to that of the graphite [17]. A boundary condition of fixed temperatures of 25 °C and 500 °C was arbitrarily applied at low- and high-temperature ends of matrix, respectively.

Fig. 3 shows temperature profiles of the model after the steady-state analysis. Two radii of the TZ were used for the straight nanotube, while a curved nanotube was modeled with a radius of curvature of 1.13 μm. In all cases, the temperature varies uniformly from the high-temperature at 500 °C to the low temperature at 25 °C. Therefore, the thermal efficiency of either the TZ or the NT curvature could not be determined from the steady-state analysis. Fig. 4 shows a temperature distribution with the transient

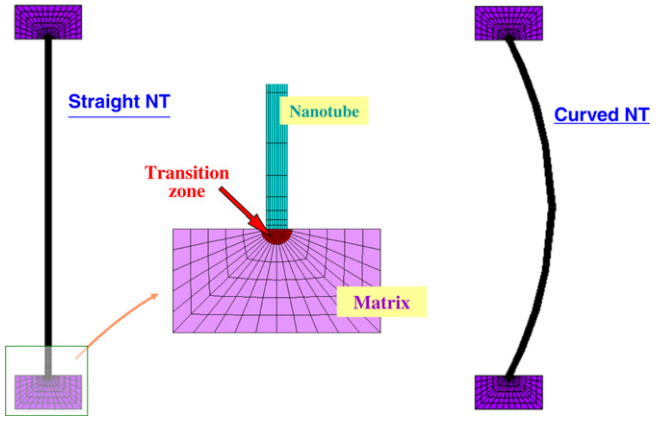

Fig. 2. Finite element model for straight and curved nanotubes embedded in matrix material through a transition zone.

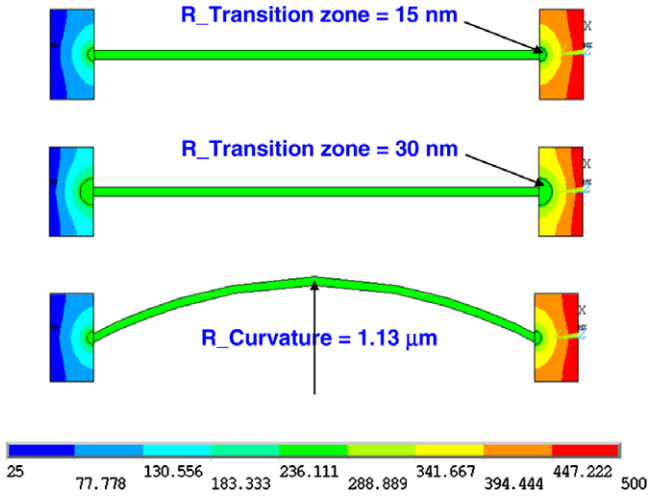

Fig. 3. Uniform temperature profiles after steady-state analysis regardless of the radius of TZ and radius of curvature of the nanotube.

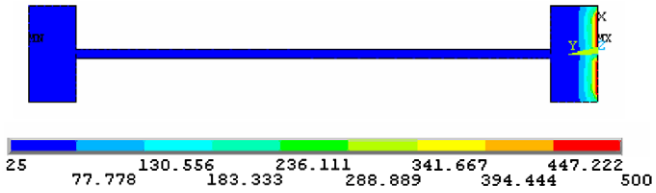

Fig. 4. Temperature profile of a transient analysis after 3 ns.

thermal analysis with the fixed temperature boundary conditions as stated above. In this model, the properties of the TZ were assumed to be the same with those of the surrounding matrix material. The temperature profile shows the instant temperature variation near the high-temperature end after a short duration of three nanoseconds, which indicated that the transient analysis potentially be used for analyzing the thermal efficiency of the TZ and NT conductivity and its curvature through a parametric study.

2.2. Parametric study

Parametric studies were conducted with the transient thermal analysis by varying parameters such as thermal conductivity of the nanotube and the TZ as well as the radius of curvature of the nanotube and the radius of the TZ. The baseline properties stated above were used if not stated explicitly in the parametric study.

2.2.1. Effect of thermal conductivity of nanotube

Firstly, the thermal conductivity of the nanotube was varied from 5 W/m K to 500 W/m K, while that of the TZ was fixed at 0.2 W/m K. The temperatures at three points in the nanotube (Points A, B and C in Fig. 5) were calculated with increase of the transient time history up to 0.3 μs. The lowest $k_{NT} = 5$ W/m K results in the largest difference in the temperatures at these points, and the increase of the k_{NT} gradually make the difference smaller.

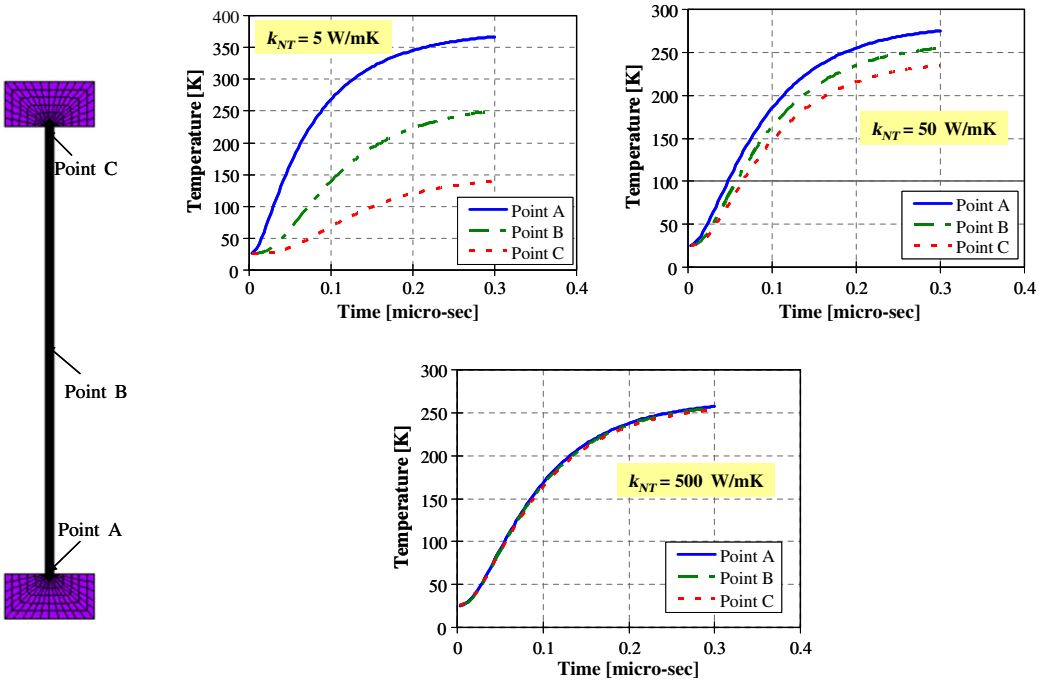

Fig. 5. Temperature increase at Points A, B and C in the nanotube against transient time with various k_{NT}.

With $k_{NT} = 500$ W/m K, the temperature difference at the three points were negligible, which indicates extremely good heat transfer. Therefore, the conductivity of the nanotube, whether it is single-walled or multi-walled nanotube, significantly affects the heat transfer efficiency.

2.2.2. *Effect of radius of curvature of nanotube*

The transient thermal analysis was conducted for the curved nanotube with three different radii of curvature, $R_{NT} = 0.52$ μm, 1.13 μm and ∞ (straight NT). With a nanotube radius of 10 nm, the ratios of the nanotube curvature to its radius were 52, 113, and ∞, respectively. The nanotubes having low (5 W/m K) and high (500 W/m K) thermal conductivities were used for the calculation, as shown in Figs. 6 and 7, respectively. The temperatures at three points (Points A, B and C) were calculated with increase of the transient time history up to 0.3 μs. Again, k_{TZ} was fixed at 0.2 W/m K. Similar to the straight nanotube, the curved nanotubes

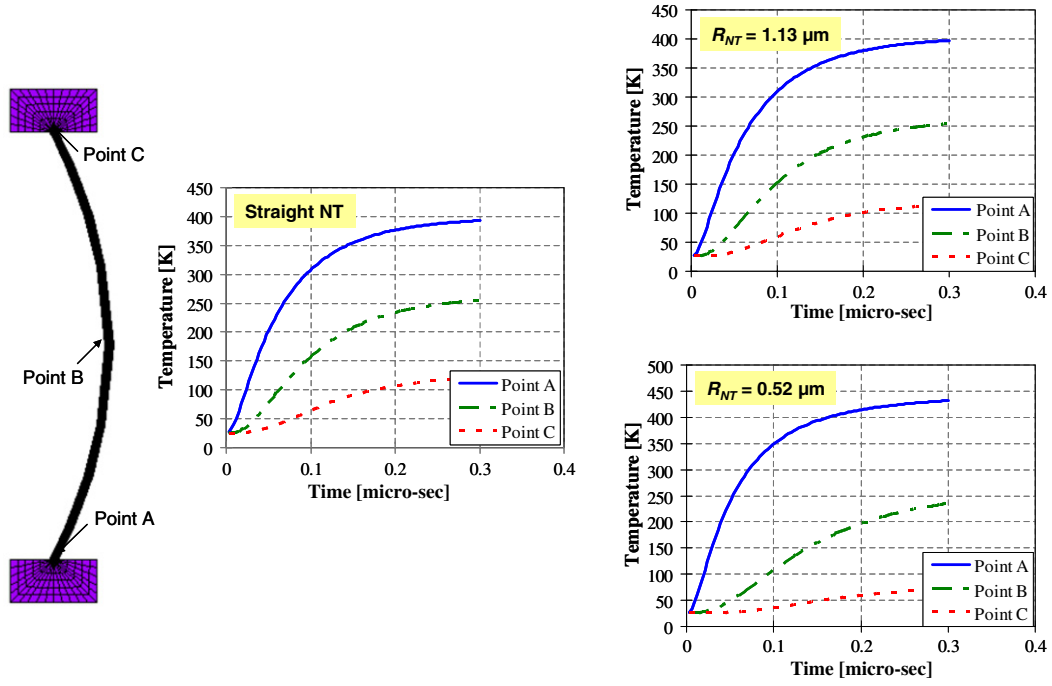

Fig. 6. Temperature increase at Points A, B and C in the straight and curved nanotubes against transient time with various R_{NT} ($k_{NT} = 5$ W/m K).

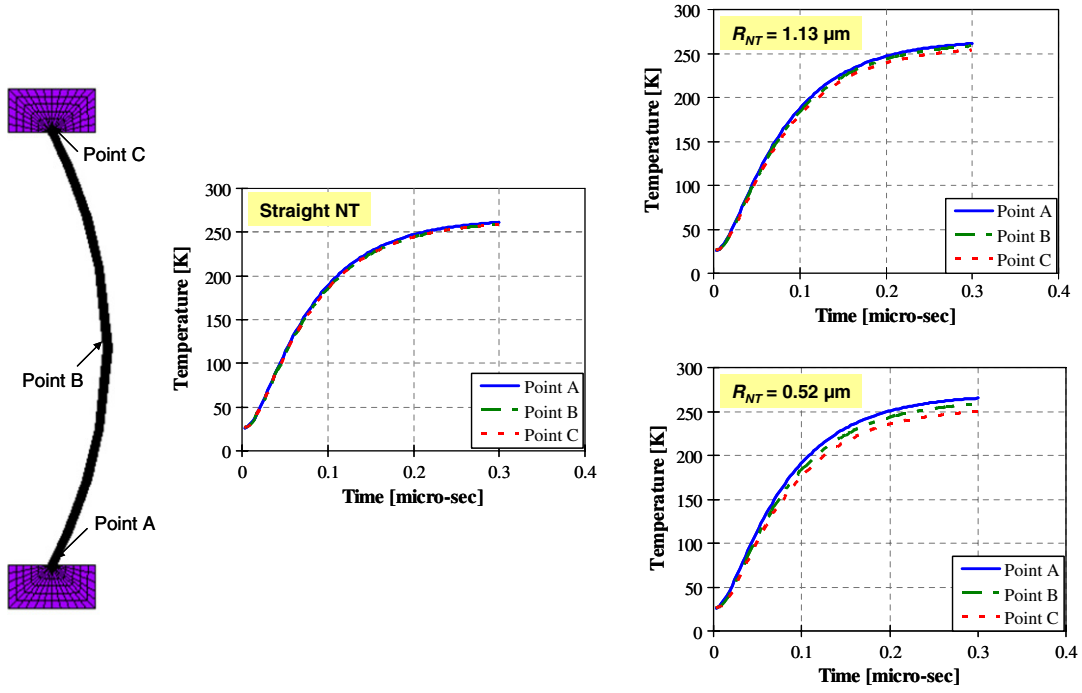

Fig. 7. Temperature increase at Points A, B and C in the straight and curved nanotubes against transient time with various R_{NT} ($k_{NT} = 500$ W/m K).

with low k_{NT} results in large difference of the temperatures at the three points, and those with high k_{NT} results in negligible difference. Furthermore, Fig. 7 shows that the curviness of the nanotube has negligible influence on the heat transfer with the high k_{NT}.

2.2.3. Effect of thermal conductivity of transition zone

The parametric study was conducted by varying the thermal conductivity of the TZ from 0.02 W/m K to 20 W/m K. The temperature at a contact point (Point A in Fig. 8) between the nanotube and the TZ was calculated with the increase of the transient time history up to 0.3 μs, as shown in Fig. 8. The lowest $k_{TZ} = 0.02$ W/m K results in the slowest heat transfer in the TZ, and the increase of the k_{TZ} gradually increases the heat transfer with the time. However, the k_{TZ} higher than 2 W/m K results in negligible temperature increase with the time. Therefore, it is necessary to achieve a good thermal transition between the nanotube and matrix material for the better heat transfer, but the improvement has a diminishing return with the improvement of k_{TZ}.

2.2.4. Effect of radius of transition zone

The radius of the TZ was varied from 0 nm to 30 nm, and the temperature increase with the time was calculated. The thermal conductivities of the nanotube and the TZ were set at 500 W/m K and 20 W/m K, respectively. As Fig. 9 shows a larger radius of the TZ with the higher thermal conductivity facilitates the heat transfer (increases the temperature) quickly. Therefore, it is desirable to introduce large volume of the high conductive TZ for the efficient thermal transfer.

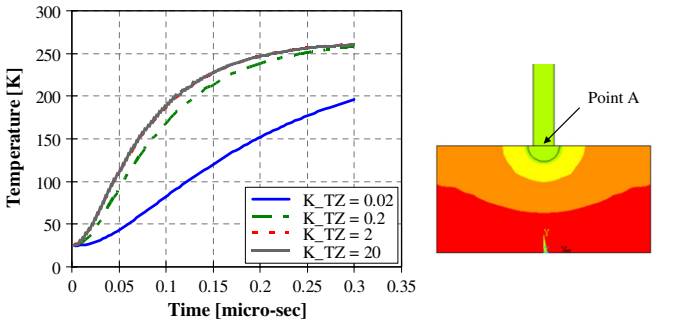

Fig. 8. Temperature increase at a contact point between the nanotube and the TZ (Point A) against transient time with various k_{TZ}.

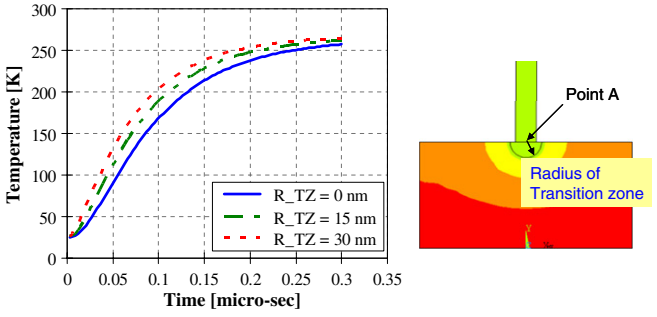

Fig. 9. Temperature increase at a contact point between the nanotube and the TZ (Point A) against transient time with various R_{TZ}.

3. Experiments

3.1. Processing

The finite element numerical study indicated that introduction of a small TZ at the MWCNT ends (i.e., at the interface of the MWCNTs and the surrounding matrix (adhesive and/or adherend materials)) of thermal conductivity higher than that of the matrix will enhance the phonon transport; hence it is expected to improve through-thickness thermal conductivity in the adhesive joints. Among many possible methods, the TZ was introduced through suitable functionalization of nanotubes and a series of metallic coatings by gold and Indium in this study.

Firstly, MWCNT films were grown on quartz substrates by chemical vapor deposition. The aligned CNT films were prepared by pyrolyzing iron(II) phthalocyanine under Ar/H_2 at 900 °C as described in detail elsewhere [18]. The diameter of the tubes was 30 nm, and the length of the MWCNT film was 30 μm. Fig. 10 shows the cross-sectional view of the as-produced MWCNT film. The vertical alignment of the nanotubes is evident from the SEM image. The samples with the MWCNT side facing upwards were dipped in a beaker containing a 10% Epon 862/W – acetone solution. The film was then kept in a vacuum oven at 60 °C for 2 h for the solvent to escape. The epoxy was then cured at 177 °C for 2 h. Fig. 11 shows the cross-sectional view of the MWCNT film infused with the epoxy. The epoxy-MWCNT film was then peeled off the quartz substrate by etching with a 10% HF solution. The nanotube tips were exposed selectively by etching the film surface with 32 watt RF oxygen plasma for 30 min. The SEM images of the film after the plasma etching are shown in Fig. 12. It can be observed from the figure that the nanotube tips are clipped due to the plasma etching. The side of the film which was previously anchored to the substrate was similarly etched in RF plasma under the above-mentioned conditions.

Next, in order to establish desirable transition zone (TZ) at the MWCNT tips, a 900-nm layer of gold was thermally evaporated on both sides of the film. Pyrolytic graphite adherend facesheets were sputter-coated with Au–Pd for 3 min. Then, a thin layer of Indium metal was melt-coated on the graphite adherend surfaces and the epoxy-nanotube film to minimize thermal resistance typically caused by surface roughness. Finally the epoxy-nanotube film was sandwiched between the graphite facesheets and fused together by heating at 175 °C to the schematic configuration shown in Fig. 1.

3.2. Measurement of thermal conductivity

The effective thermal conductivity of the adhesive joint system were measured by measuring thermal diffusivity

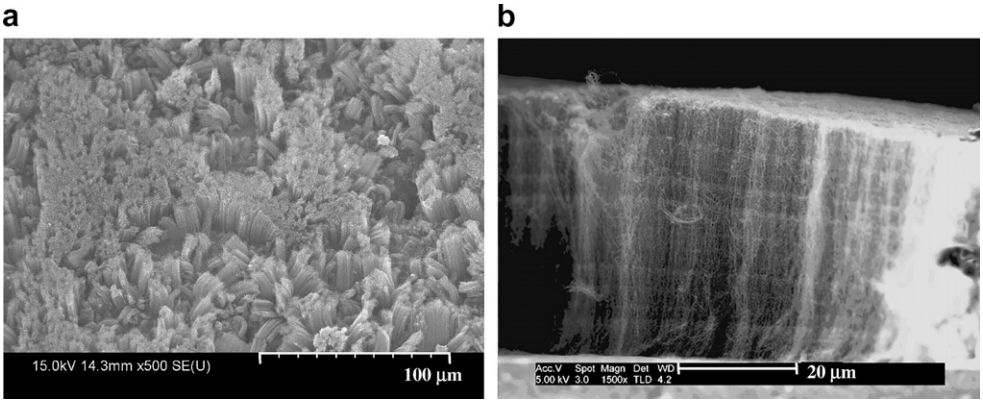

Fig. 10. SEM micrograph of cross-sectional view of as-produced MWCNT film (nanograss).

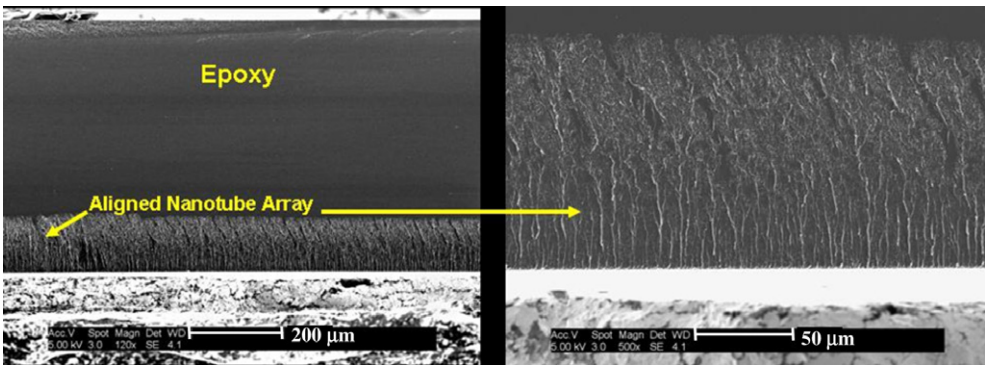

Fig. 11. SEM micrograph of cross-section of epoxy-infused MWCNT film before plasma etching.

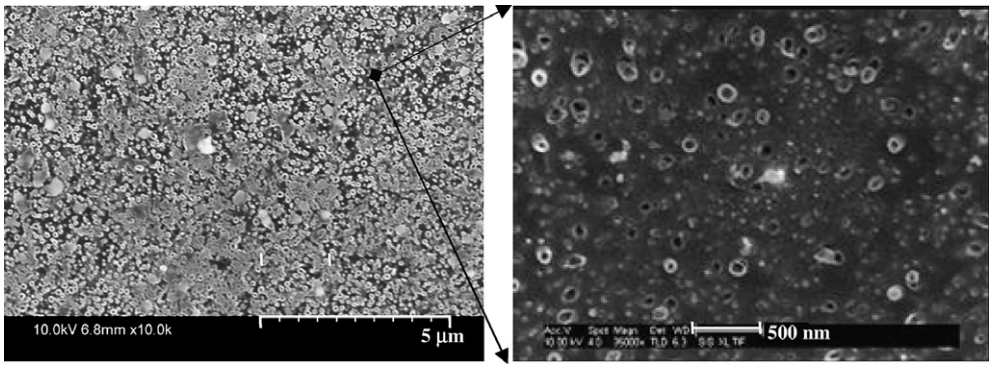

Fig. 12. SEM micrograph of adhesive film with MWCNT tips exposed after plasma etching (View normal to MWCNT film plane).

using a laser flash (or heat pulse) technique. The measurement was made using a Netzsch laser flash apparatus [19] under nitrogen purge. The laser flash technique allows measuring the thermal diffusivity of solid materials over a temperature range from −180 °C to 2000 °C. The laser flash technique consists of applying a short duration (less than 1μs) of heat pulse to one face of the parallel-sided sample and monitoring the temperature rise on the opposite face as a function of time. The temperature rise was monitored with an infrared detector. The specific heat (C_p) was also measured with the same laser flash apparatus by comparing the temperature rise of the sample to the temperature rise (ΔT) of a reference sample of known specific heat tested under the same conditions. The temperature rise was recorded during the diffusivity measurement, so the specific heat can be calculated from the same data with a suitable calibration. Assuming the laser pulse energy and its coupling to the sample remain unchanged between the samples, the heat capacity becomes $C_p = (m\ C_p\Delta T)_{\text{reference}}/(m\Delta T)_{\text{sample}}$, where m is mass. The density (ρ) was calculated by measuring the weight and the volume of the samples.

With the measurement of the thermal diffusivity (h), the heat capacity (C_p) and the density (ρ), the thermal conductivity (K_z) was then calculated as $K_z = \rho C_p h$. The thermal conductivity of the graphite facesheet and the neat epoxy were also calculated with the same method. Note that all the thermal conductivity measurements made in this study were performed at room temperature. The laser voltage used was 1826 V with a gain of 50 and an orifice area of 78.54 mm^2. A diffusivity model used for fitting the experimental data was a Cowan + pulse correction model and the correlation coefficient for the data fit was 0.99864. The measurement values for the graphite facesheet, the epoxy and the device with and without the CNTs are listed in Table 1, and the thermal conductivity values are shown in Fig. 13. A theoretical value of the $k_{\text{NT}} = 2000$ W/m K is also shown in the figure. The thermal conductivities of the graphite facesheet, the epoxy adhesive and the present joint device were 447.7, 0.275 and 250.4 W/m K respectively. The joint device without using the vertically aligned CNTs yielded the thermal conductivity of 0.790 W/m K. It should be noted that the present joint system has the metallic interface of Au and Pd instead of the polymeric interface between the adherends and the adhesive layer. The metallic interface lowered the phonon scattering at the interface and yielded the relatively high K_z compared with the similar study by Huang et al. [15].

Table 1
Measured values of density, heat capacity and thermal diffusivity of epoxy, graphite and joint device, and their calculated thermal conductivity

Material	Density (ρ) [g/cm^3]	Heat capacity (C_p) [J/g K]	Thermal diffusivity (h) [mm^2/s]	Thermal conductivity (K_z) [W/m K]
Epoxy	1.106	1.200	0.207	0.275
Graphite	1.800	0.859	289.6	447.7
Device (without NTs)	1.200	0.043	15.32	0.790
Device (with NTs)	1.820	0.151	911.3	250.4

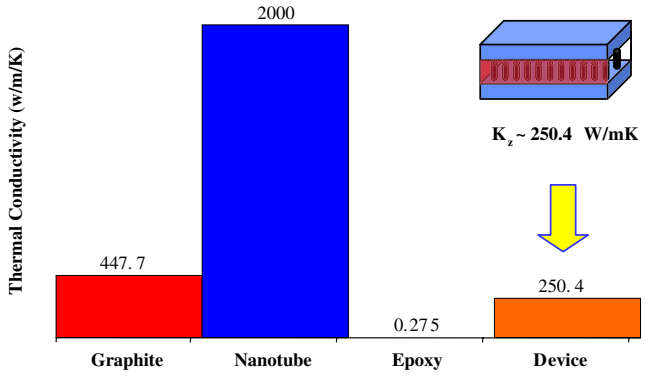

Fig. 13. Comparison of measured through-thickness thermal conductivities of the graphite adherend (facesheet), a MWCNT (theoretical), epoxy adhesive and the adhesive joint device with the vertically aligned MWCNT.

4. Summary and discussion

A concept of incorporating aligned conductive phase (MWCNT) in the adhesive layer has been demonstrated to enhance the through-thickness thermal conductivity in the adhesively bonded joints. The key parameters for improving the through-thickness thermal conductivity in

the adhesive joint, identified though the numerical study, are (1) the improvement of the thermal conductivity of the aligned nanotubes as well as (2) the thermal conductivity and the size of the TZ near the nanotube ends and the adherend surfaces. Therefore, the thermal contact of the conductive phase with the adherent surfaces needs to be established in order to achieve the desirable thermal transport through the thickness. Further, acoustic impedance mismatch at the interface (TZ) needs to be minimized to minimize the phonon scattering to maximize thermal transport. This theoretical observation was realized experimentally by using aligned MWCNTs (nanograss), surface functionalization by Au on the nanotube ends and by Au–Pd on adherend surfaces and introduction of the TZ by Indium.

The measurement of the through-thickness thermal conductivity of the adhesive joint was conducted by the thermal diffusivity method using the laser-flash method. The measured through-thickness thermal conductivity of the joint configuration of aligned MWCNT infused with adhesive, using pyrolitic graphite face sheet was over 250 W/m K, which is a significant improvement of the through-thickness thermal conductivity compared with the one without the aligned MWCNT. $k_z \sim 250$ W/m K supersedes the through-thickness thermal conductivity requirement of the adhesive joints for space structures by an order of magnitude. However, it should be noted that since k_z of composite facesheets is much lower than that of pyrolitic graphite facesheets, k_z of the same joint configuration using the composite facesheets is expected to be lower than 250 W/m K.

References

[1] Iijima S. Helical microtubules of graphitic carbon. Nature (London) 1991;354(6348):56–8.
[2] Frank S, Poncharal P, Wang ZL, De Heer WA. Carbon nanotube quantum resistors. Science 1998;280(5370):1744–6.
[3] Kim P, Lieber CM. Nanotube nanotweezers. Science 1999;286(5447):2148–50.
[4] Berber S, Kwon Y-K, Tomanek D. Unusually high thermal conductivity of carbon nanotubes. Phys Rev Lett 2000;84(20):4613–6.
[5] Ghosh S, Sood AK, Kumar N. Carbon nanotube flow sensors. Science 2003;299(5609):1042–4.
[6] Baughman RH, Cui C, Zakhidov AA, Iqbal Z, Barisci JN, Spinks GM, et al. Carbon nanotube actuators. Science 1999;284(5418):1340–4.
[7] Frackowiak E, Beguin F. Electrochemical storage of energy in carbon nanotubes and nanostructured carbons. Carbon 2002;40(10):1775–87.
[8] Clifford JP, John DL, Castro LC, Pulfrey DL. Electrostatics of partially gated carbon nanotube fets. IEEE Trans Nanotechnol 2004;3(2):281–6.
[9] Che J, Cagin T, Goddard WA. Thermal conductivity of carbon nanotubes. Nanotechnology 2000;11(2):65–9.
[10] Kim P, Shi L, Majumdar A, McEuen PL. Thermal transport measurements of individual multiwalled nanotubes. Phys Rev Lett 2001;87(21):215502.
[11] Xie H, Lee H, Youn W, Choi M. Nanofluids containing multiwalled carbon nanotubes and their enhanced thermal conductivities. J Appl Phys 2003;94(8):4967–71.
[12] Xue QZ. Model for effective thermal conductivity of nanofluids. Phys Lett A 2003;307(5-6):313–7.
[13] Biercuk MJ, Llaguno MC, Radosavljevic M, Hyun JK, Johnson AT, Fischer JE. Carbon nanotube composites for thermal management. Appl Phys Lett 2002;80(15):2767–9.
[14] Liu CH, Huang H, Wu Y, Fan SS. Thermal conductivity improvement of silicone elastomer with carbon nanotube loading. Appl Phys Lett 2004;84(21):4248–50.
[15] Huang H, Liu C, Wu Y, Fan S. Aligned carbon nanotube composite films for thermal management. Adv Mater 2005;17(13):1652–6.
[16] Cahill DG, Ford WK, Goodson KE, Mahan GD, Majumdar A, Maris HJ, et al. Nanoscale thermal transport. J Appl Phys 2003;93(2):793–818.
[17] Masarapu C, Henry LL, Wei B. Specific heat of aligned multiwalled carbon nanotubes. Nanotechnology 2005;16(9):1490–4.
[18] Wang QH, Corrigan TD, Dai JY, Chang RPH, Krauss AR. Field emission from nanotube bundle emitters at low fields. Appl Phys Lett 1997;70(24):3308–10.
[19] E-thermal, 2007, <http://www.e-thermal.com>.